Heterogeneous & Homogeneous & Bio- & Nano-
CHEMCATCHEM
CATALYSIS

# Accepted Article

**Title:** Selective glucose to fructose isomerization over modified zirconium UiO-66 in alcohol media

**Authors:** Matheus Dorneles de Mello and Michael Tsapatsis



**To be cited as:** *ChemCatChem* 10.1002/cctc.201800371

**Link to VoR:** http://dx.doi.org/10.1002/cctc.201800371

A Journal of
ChemPubSoc Europe

WILEY-VCH

www.chemcatchem.org

WILEY-VCH

FULL PAPER

# Selective glucose to fructose isomerization over modified zirconium UiO-66 in alcohol media

Matheus Dorneles de Mello,[a] and Michael Tsapatsis*[a]

**Abstract:** Modulated zirconium metal-organic framework UiO-66 is shown to catalyze the isomerization of D-glucose to D-fructose in alcohol media. Fructose selectivity can change depending on solvent choice. We hypothesize that the difference in selectivity is due to a combined effect of adsorption and solvation effects, which may lead to the high formation of alkyl-glucosides in depletion of fructose when methanol or ethanol are used. A fructose selectivity of 72 % at 82 % glucose conversion in 1PrOH was achieved. The reaction mechanism was investigated using nuclear magnetic resonance spectroscopy. We demonstrate that UiO-66 isomerizes glucose to fructose via intramolecular C2-C1 hydride transfer. In addition, we show that modulated UiO-66 is a highly active and stable catalyst at the reaction conditions, showing great potential for other sugar reactions.

## Introduction

Biomass is an alternative carbon source to fossil fuels for the production of platform chemicals[1], such as 5-hydroxymethylfurfural (HMF), which can be used as polymer precursors and in the synthesis of pharmaceuticals.[2–4] One of the routes available to produce HMF passes through the hydrolysis of cellulose to glucose, followed by glucose isomerization to fructose, and finally dehydration of fructose to HMF.[5–7] Glucose is the most abundant and cheapest monosaccharide available. However, the industrial enzyme-catalyzed glucose isomerization process[8,9] due to thermodynamic limitations present in aqueous media[10], its high cost and low catalyst stability, offers opportunities for novel processes based on non-enzymatic routes.

Considerable effort has been devoted in the past years to improve yields and selectivity in fructose by investigation of different systems, including homogeneous acids and bases, and heterogeneous catalysts. Davis and co-workers introduced the use of substituted BEA zeolites as efficient Lewis acid catalysts for glucose isomerization. Since then, Sn-BEA and several variations have been deeply investigated[11–15], providing a wide range of possibilities regarding activity, selectivity, and even reaction mechanisms depending on the catalyst-reaction media pair under study.

It is accepted that glucose isomerization to fructose on Lewis acid sites occurs via a Meerwein–Ponndorf–Verley-Oppenaher (MPVO) mechanism that involves the concerted reduction of a carbonyl and the oxidation of adjacent alcohol through a hydride transfer.[16,17] First, glucose diffuses from the external liquid phase onto the active sites, followed by adsorption and ring-opening of glucose on these sites. All these steps are assumed to be quasi-equilibrated.[14] After that, coordination of glucose to an active site leads to the C2 to C1 hydride transfer, which is assumed to be the rate-determining step.[18] Fructose is then desorbed and diffuses back to the external fluid phase.

Another possible primary product in the reaction is mannose, the epimer of glucose. When sodium was incorporated into the active site of Sn-BEA[12], or when borates were used as catalysts[19], glucose epimerized to mannose through an intramolecular carbon shift, known as the Bilik reaction. It is also possible to form mannose from a reverse 1,2-hydride transfer from fructose, as it was observed for $CrCl_3$ and other metal halides as catalysts.[20]

As an attempt to find new heterogeneous catalysts with Lewis acidity for glucose isomerization, metal-organic frameworks (MOFs) have drawn significant attention due to their high tunability and density of active sites.[21] MOFs are composed of metal clusters connected by organic linkers, which can have their characteristics modified upon different choices of metals and linkers.[22] However, an obstacle for the applications of MOFs can be their limited stability.[23]

The zirconium MOF UiO-66[24] is one of the MOFs with highest reported stability, both chemical and thermal.[23,25,26] The Zr clusters can act as Lewis acid sites, as it was observed for the cyclization of benzaldehyde and aldol condensation.[27–30] A modified UiO-66 with Brønsted acid sites has been studied for glucose isomerization to fructose in water, achieving high selectivity at 48 % glucose conversion.[31] A similar synthesis procedure was used to make an active catalyst for fructose dehydration to HMF, showing high activity and stability at reaction conditions.[32]

As a tool to increase activity, acid modulation can be used to control porosity and shape-selectivity.[33] A modulator acts as a competitor to the ligands for the metal clusters. In this matter, it should have similar chemical properties to the linker. The use of modulation creates defects in the framework, which can be just due to linker substitution or to the removal of an entire cluster. Recently, acid modulation was comprehensively investigated by Lillerud and co-workers to elucidate the creation of these defects in UiO-66. It was concluded that the defect-formation is mainly due to missing-clusters and correlates well with the acidity of the modulator.[34]

Here we use the acid modulation technique to create an efficient UiO-66 catalyst for sugar isomerization reactions. We report high yields of fructose and the effects of the solvent on selectivity. The reported yields are comparable to the highest ones obtained using other microporous and mesoporous materials.

[a] M. Dorneles de Mello, Prof. M. Tsapatsis
Department of Chemical Engineering and Materials Science
University of Minnesota
421 Washington Avenue SE
Minneapolis, MN 55455 (USA)
E-mail: tsapatsis@umn.edu

Supporting information for this article is given via a link at the end of the document.

## Results and Discussion

The defect-free and modulated samples were initially characterized to check for their structural and physicochemical properties. The XRD patterns presented in Figure S1 match those simulated for UiO-66, indicating that the material was successfully synthesized, and the structure remained intact upon activation at 200 °C.[24,33] As a result of modulation, a prohibited reflection at 5° was identified and assigned to the formation of UiO-66 in its reo-phase (with one missing cluster per unit cell).[34] A peak at 14° could also be identified in the XRD pattern of UiO-66-Id and is usually attributed to a prohibited reflection due to the presence of guest molecules inside the framework, most likely DMF.[24,33] The mentioned feature is absent from the pattern of UiO-66-Fm, indicating that the washing and activation procedures were able to remove the solvent and non-reacted linkers from the framework efficiently.

Figure S2a displays the Ar adsorption-desorption isotherms of the samples. The isotherms show a type II pattern. Two different trends in Ar uptake were observed for UiO-66-Id at $10^{-4}$ P/Po and at $10^{-2}$ P/Po, attributed to the filling of the micropores of 4 and 6 A, respectively. Acid modulation led to an increase in Ar uptake, mostly after $10^{-2}$ P/Po, associated with the formation of larger pores due to the introduction of the missing-clusters defects.[34] Figure S2b displays the pore size distribution, and Table S1, the surface area and pore volume of the samples. The obtained values are similar to others previously reported for UiO-66.[25,35,36] As expected, modulation increased the pore volume and the surface area.

The TGA traces of UiO-66 are presented in Figure S3. Three regions can be identified: (1) Adsorbate volatilization such as $H_2O$ (25 to 100 °C). (2) Solvent removal and dehydroxylation of Zr clusters (100 to 250 °C). (3) Loss of modulator (250 to 400 °C). (4) Framework decomposition (400 to 540 °C).[25] From ICP results, the modulated sample (UiO-66-Fm) presented a smaller carbon to zirconium ratio in contrast to the defect-free one (UiO-66-Id), indicating the formation of defects (Table S2). The defect-free sample presented a higher C/Zr atomic ratio than the theoretical value (8.7 instead of 8.0), which is most likely due to the presence of guest molecules in the framework, also observed by XRD.

Once the presence of defects was identified, it was crucial to identify the nature of these defects. Two possibilities were investigated considering previous reports for UiO-66 structures: OH groups distribution and presence of organic modulator.[25,37] The $OH^-/H_2O$ distribution in the samples was investigated by DRIFTS (Figure S4), and we could identify the presence of two bands at 3670 and 3635 $cm^{-1}$. The first one is attributed to $\mu_3$ bridging OH groups, typical of UiO-66, and the second band is associated with the formation of a new type of a bridged $H_2O$/OH group bonded to Zr sites.[37] Analyzing the 1800 – 1400 $cm^{-1}$ region of the spectra can provide information on the types of organic molecules present in the framework. The peaks at 1667 and 1446 $cm^{-1}$ are assigned to OCO asymmetric and symmetric stretching, respectively, while the peaks at 1598,1509 and 1381 can be assigned to the C=C of the carboxylic ring.[38] Upon modulation, a new peak appears at 1460 $cm^{-1}$, what is an indication of the presence of an OCO stretching of a different carboxylic group, most likely formate. The region from 700 to 500 $cm^{-1}$ refers to the different Zr-O stretching modes mixed with OH and C-H bending modes.

We also applied the dissolution NMR technique (Figure S5) to obtain the distribution/types of carboxylates in the sample. UiO-66-Id shows two proton signals at 4.8 and 7.8 ppm, assigned to $D_2O$ and to the symmetric protons in the aromatic ring of terephthalic acid (which appear as a singlet) after dissolution. UiO-66-Fm presented a new peak at 8.4 ppm, attributed to the proton of the formate group ($HCOO^-$), thus confirming that formate was incorporated into the framework as a compensating ligand upon modulation. SEM images showed crystals of around 200 nm for UiO-66-Id and around 100 nm for UiO-66-Fm with an octahedral shape (Figure S6).

TGA results alone cannot distinguish between types of defects (missing-cluster or missing-linkers). We combined ICP, NMR and TGA results to obtain the experimental molecular formula of the modified material, displayed in Table S3.

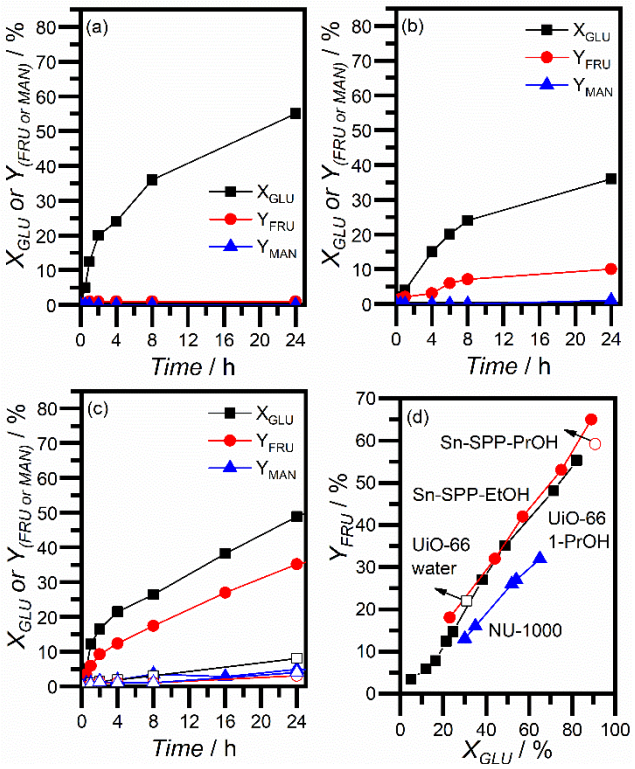


**Figure 1.** Glucose isomerization profiles for UiO-66-Fm in (a) MeOH, (b) EtOH, (c) 1-PrOH (open symbols refer to UiO-66-Id), and (d) performance comparison of UiO-66-Fm in 1-PrOH (black), Sn-SPP in EtOH (red)[39], Sn-SPP in 1-PrOH (red circle, open), NU-1000 in EtOH[40] (blue), and UiO-66-$SO_3H$ in water[31] (black square, open). Reaction conditions: 0.007 g of catalyst, 5 mL of solvent, 0.04 g of D-glucose, 90 °C, 600 rpm.

The combination of these results supports the evidence of the missing-cluster defects provided from XRD (broad peak at 5°) and adsorption isotherms. In an extensive study using

experimental and simulated adsorption data on UiO-66, Lillerud and co-workers concluded that the increase in volume uptakes for modulated samples could not be just to missing-linkers, but to missing-cluster defects.[34]

The catalytic activity of UiO-66 for glucose isomerization was investigated following a two-step batch mode procedure using different alcohols as solvents. This approach was introduced by Saravanamurugan et al. and involves the isomerization of glucose to fructose, which reacts with the solvent to form the respective alkyl fructoside.[41] In a second reaction step, water is added to hydrolyze the fructoside back to fructose. The two-step method used in this work allows for higher yield at the expense of a two-step reaction. Although a detailed techno-economic analysis has not been performed regarding the competitiveness of this approach, given that processing costs are a small fraction of the glucose cost[42], improvements in selectivity are expected to be advantageous despite the addition of any processing costs. Fructose yields at different glucose conversions after reaction with UiO-66-Fm (or UiO-66-Id) are displayed in Figure 1. The modulated UiO-66 exhibited much higher activity than the defect-free one (compare closed and open symbols in Figure 1c), indicating that the larger pores present in UiO-66-Fm are necessary for glucose to gain access to catalytic sites. The carbon balances (accounting for glucose, fructose, and mannose) close at around 85 %, indicating the formation of side products, such as retro-aldol products. The solution remained colorless after the reaction, indicating that dehydration and condensation byproducts were not formed in significant amounts.[12,43]

The data presented in Figure 1(a-c) show that different fructose selectivities can be obtained depending on the alcohol choice as a solvent for UiO-66-Fm. The use of methanol completely suppressed the formation of fructose. As the alkyl chain length of the solvent increased, the yield in fructose improved. A maximum of 56 % fructose yield at 82 % glucose conversion was achieved for the reaction in 1-propanol. UiO-66-Fm shows a fructose selectivity and yield comparable to the one previously reported for Sn-SPP in ethanol[39] (and 1-propanol, in this work), higher than that obtained for another zirconium MOF, NU-1000[40], and similar to the recently reported for UiO-66-$SO_3H$ in water[31] (Figure 1d).

To confirm that the reaction is catalyzed by the MOF, we performed a hot filtration test, in which we filtered off the catalyst after 2h of reaction. The filtrate was left at the same reaction conditions for another 22 h. As shown in Figure S7, the termination of reaction in the filtrate attests to the absence of active leached species into the solution. We also evaluated the catalyst recyclability. UiO-66-Fm retained its catalytic activity after 3 reaction cycles (Figure S8), presenting similar conversion and selectivity as the fresh material. A small decrease in conversion after the third cycle was observed, most likely due to blockage of a few active sites after the reaction. Characterization of the spent catalyst showed no apparent changes in crystalline structure or morphology after the reaction. A small decrease in Ar uptake was observed, probably due to trapped chemicals inside the framework (see Figures S9-S11).

The glucose isomerization mechanism was investigated by reacting isotopically labeled glucose with UiO-66-Fm. Resonances at δ = 95.6 ppm and 92 ppm are characteristic of the C1 glucose peaks of β-pyranose and α-pyranose, respectively. [44] $^{13}C$ NMR spectra after reactions with 1-propanol were obtained using two different labeled glucose solutions: D-[13C-C1, 1H-C2]-glucose or D-[13C-C1, 2H-C2]-glucose. The reaction of D-[13C-C1, 1H-C2]-glucose leads to the appearance of three singlets at δ = 63.5, 62.3 and 61.3 ppm, assigned to β-pyranose, α-furanose and β-furanose forms of C1 carbon of fructose, respectively (Figure 2b). However, low-intensity triplets arise upon use of D-[13C-C1, 2H-C2]-glucose for reaction, providing evidence that the deuterium at C2 of glucose has shifted to C1 of fructose through an intramolecular hydride transfer. The triplets are formed due to the coupling between deuterium and carbon, according to a loss of nuclear Overhauser effect.[20] The $^{1}H$ NMR spectrum of the solution after reaction supports the hypothesis of hydride transfer by the disappearance of the resonance at δ = 3.45 ppm, which corresponds to a proton bonded to C1 of fructose (Figure S12). The results confirm that UiO-66-Fm catalyzes glucose isomerization to fructose through 1,2-hydride transfer, the same mechanism reported for Sn-BEA and other materials.[15,45]

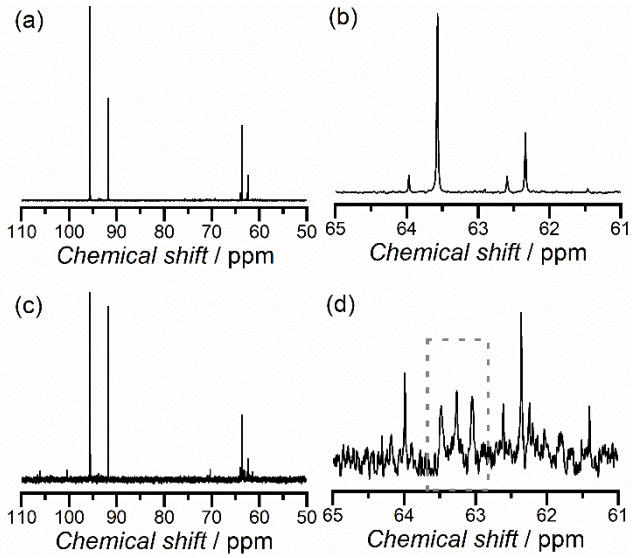


**Figure 2.** $^{13}C$ NMR spectra of hydrolyzed solution after reaction of D-[13C-C1, 1H-C2]-glucose with UiO-66-Fm in 1-PrOH: (a) Complete spectrum and (b) fructose region. Reaction of D-[13C-C1.2H-C2]-glucose with UiO-66-Fm in 1-PrOH: (c) Complete spectrum and (d) fructose region.

Spectra in Figure 2 show low-intensity peaks assigned to C1 of mannose (δ =93.9 and 93.5 ppm). No peaks of C2 of mannose (δ =71.1 and 70.5 ppm) were detected. These results suggest that mannose is being formed through a reverse 1,2-hydride transfer from fructose and not from a Bilik reaction mechanism, which involves intramolecular carbon shift. The formation of mannose through a reverse 1,2-hydride transfer from fructose was also observed for Sn-BEA zeolite.[20] The mechanistic results are in alignment with the observed behavior

in our reaction data in 1-propanol, in which an increase in mannose yield is observed as the reaction proceeds (Figure S13).

The initial step in glucose isomerization to fructose using Sn-BEA is assumed to be the adsorption of the sugar at the metal center. To determine if a similar pathway is followed using UiO-66, the adsorption of glucose and fructose into UiO-66-Fm were investigated. Adsorption isotherms of glucose and fructose from their solutions in methanol, ethanol, and 1-propanol are presented in Figure 3a. Fructose shows higher adsorption than glucose in all tested solvents. Moreover, as the alkyl chain of the solvent increases, the adsorption capacity of both sugars decreases, suggesting a weaker interaction between the sugars and the adsorption sites. A glucose adsorption isotherm on UiO-66-Id (Figure S14) showed no adsorption, which is an indication that the sugar does not have access to the pores. To further support this hypothesis, an Ar adsorption isotherm of UiO-66-Fm after glucose adsorption showed a decrease in Ar uptakes in the $P/P_o$ range between $10^{-4}$ to 1, with a decrease in pore sizes between 6 and 15 A (Figure S15).

Next, we investigated by $^{13}C$ Solid-state NMR whether the sugars adsorption occurs via ring opening (Figure 3b). The spectrum of the UiO-66-Fm sample shows three main resonances at 171, 132 and 128.9 ppm, assigned to the carbonyl, quaternary, and aromatic carbons of terephthalic acid on the framework.[46] Resonances in the regions between 200-180 and 85-65 ppm, and at 112 ppm and 58 ppm were identified as sidebands, confirmed by experiments at different spinning rates (Figure S16). Spectra obtained from glucose and fructose adsorbed into UiO-66-Fm show the appearance of bands at 70-60 ppm, indicating that the sugars are adsorbed in a cyclic configuration. There is some overlapping between the sugar resonances and those attributed to sidebands. Bands at 205 ppm or 214 ppm are assigned to the keto carbonyl carbon of the acyclic forms of glucose and fructose, respectively.[47] Bermejo-Deval et al.[12] demonstrated the presence of glucose and fructose in open form into Sn-Beta zeolite but reported that only about 5 % of the sugar adsorbed was in open form. Van der Graaff et al.[48] also followed glucose isomerization through $^{13}C$ solid-state NMR using Sn-Beta as catalyst and could not observe sugars in acyclic form. The absence of the referred bands in our NMR data could also be to very low sugar adsorption in an acyclic form, which cannot be detected when compared with the high intensity of the signals from the framework itself and the sugars in cyclic form.

Qian and Wei[49] reported using ab initio molecular dynamics simulations that it is possible for glucose to isomerize to fructose without ring-opening. However, their calculations considered a homogeneous aqueous system. Tang et al. reported that Sn-Beta and Zr-Beta were able to catalyze the ring-opening hydration of epoxides showing low apparent activation energies.[50] A similar conclusion was obtained by Tang et al.[51], who investigated the mechanism of glucose isomerization in water catalyzed by $AlCl_3$. The authors were able to observe by ATR that the mutarotation of glucose occurs faster in the presence of the catalyst, but could not observe direct evidence for ring-opening, arguing that this step could be very fast.

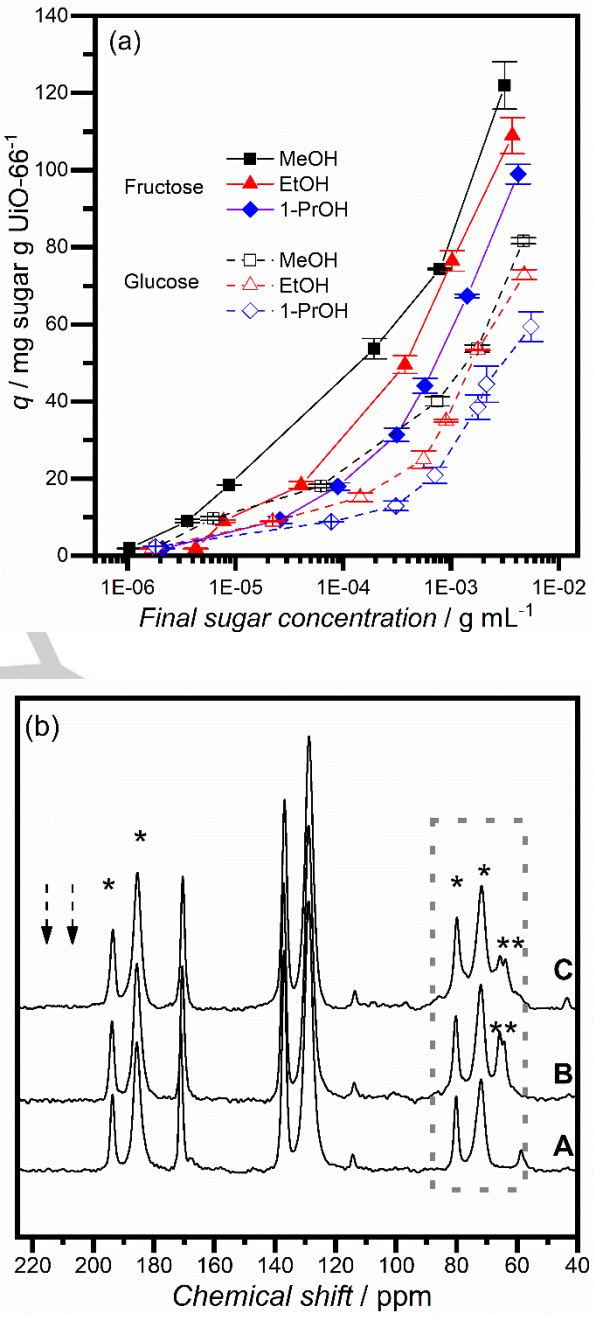


**Figure 3.** (a) Adsorption isotherms of glucose (dashed lines) and fructose (solid lines) on UiO-66-Fm in different solvents. (b) $^{13}C$ Solid-State NMR spectra of (A) pure UiO-66-Fm, (B) glucose, and (C) fructose adsorbed on UiO-66-Fm from 1-PrOH. * Refers to spinning sidebands. ** refers to bands due to sugar adsorption. Arrows indicate the chemical shifts of expected acyclic forms of glucose (205 ppm) and fructose (214 ppm).

Although we could not observe the ring-opening of glucose in our $^{13}C$ solid-state NMR experiments, it is more

likely that, at the reaction conditions, the Lewis-acid catalyzed hydride transfer is occurring on the Zr sites of UiO-66-Fm after a quick ring-opening step.

Our results show a prominent effect of the solvent on fructose selectivity. To identify what causes these differences, glucose isomerization with D-[13C-C1, 1H-C2]-glucose was further carried out in the presence of UiO-66-Fm to help with the identification of byproducts (Figure 4). $^{13}C$ NMR analysis of the reaction solutions revealed high-intensity carbon signals corresponding to the formation of methyl-glucosides and ethyl-glucosides[52] (above 110 ppm), but no formation of propyl-glucosides from glucose in 1-propanol after hydrolysis. Propyl-glucosides were identified before the hydrolysis step in small quantities but were readily hydrolyzed. Signals attributed to alkyl-fructosides (around 58 to 60 ppm) were also identified before hydrolysis (Figure S17). The solvolysis reaction of either is assumed to occur through an $SN_2$ mechanism.[53] Therefore, it is reasonable to expect that bulkier leaving groups would favor the hydrolysis of glucosides and fructosides in 1-propanol.

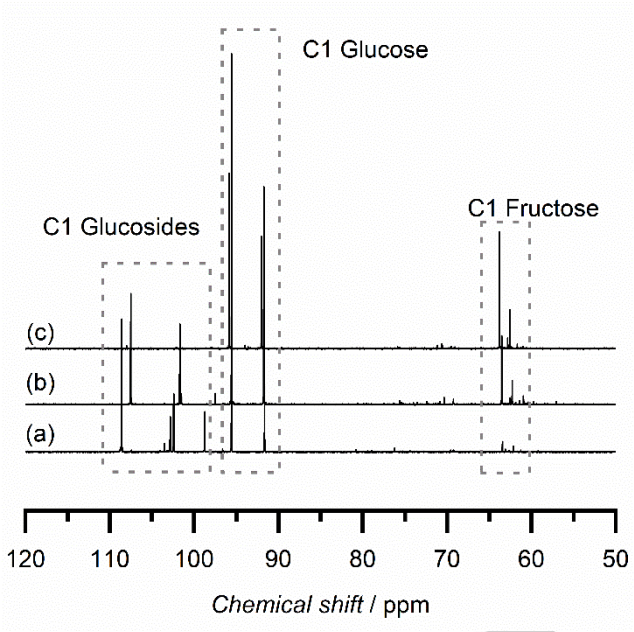


**Figure 4.** $^{13}C$ NMR spectra of hydrolyzed solution after reaction of D-[13C-C1, 1H-C2]-glucose with UiO-66-Fm in (a) MeOH, (b) EtOH, and (c) 1-PrOH.

Altogether, the data point out that isomerization through an intramolecular hydride transfer mechanism is preferred over the ketalization reaction to glucosides when using 1-PrOH as solvent.

The strong adsorption of glucose from methanol or ethanol favors the interaction of the sugar with the Brønsted acidic bridged OH group coupled with the high polarizability of methanol and ethanol could affect the proper coordination of glucose to the active site needed to yield fructose, yielding the formation of alkyl-glucosides, instead. A weaker interaction between framework and sugar, and between sugar and solvent yields more fructose. Therefore, it is reasonable to assume that there is a synergistic effect between the Lewis and Brønsted sites on UiO-66-Fm that are responsible for high fructose yields in 1-PrOH. Saravanamurugan et al.[52] reached a similar conclusion when screening commercial zeolites of various acidities for glucose isomerization.

## Conclusions

We evaluated the catalytic activity of modulated UiO-66 for glucose isomerization to fructose in different solvents. Modulated UiO-66 provides access to sugar molecules to its interior pore space and is a stable catalyst for reactions involving sugar isomerization and ketalization. It was demonstrated that glucose is converted to fructose via an intramolecular 1,2-hydride transfer mechanism. The use of different solvents (methanol, ethanol, propanol) leads to noticeable changes in fructose selectivity, with the highest values obtained in 1-PrOH (fructose and mannose selectivity of 72 % and 10%, respectively, were achieved at 82 % glucose conversion in 1-PrOH).

## Experimental Section

Catalyst synthesis and characterization: UiO-66 was synthesized by a solvothermal method. In a typical procedure, $ZrCl_4$ (1.70 g, 7.30 mmol) and 10 mL of formic acid (modulator) were dissolved in a mixture of 120 mL of DMF and 0.4 mL of $H_2O$ by stirring for 5 min. The linker precursor benzene 1,4-dicarboxylic acid (1.56 g, 9.39 mmol) was then added to the solution and dissolved by stirring for 5 min. The homogeneous solution was then poured into Teflon autoclave liners and placed in an oven at 120 $^oC$ under static conditions for 72h. The obtained white powder was isolated by centrifugation after cooling to room temperature and washed in DMF overnight at 70 $^oC$ under stirring. The material was further washed with DMF three times to remove unreacted precursors and with ethanol for two times to remove DMF. Then, the powder was dried at room temperature overnight. Catalysts were activated under vacuum by heating at 200 $^oC$ for 14h. A defect-free UiO-66 was also synthesized for comparison. In that case, the synthesis procedure was similar except for the absence of modulator, oven temperature (220 $^oC$) and time (24h). The catalysts prepared were denoted as UiO-66-Id (defect-free, without modulator) and UiO-66-Fm, modulated sample. Elemental composition was determined by inductively coupled plasma atomic emission spectrometry (ICP). Powder X-ray diffraction (PXRD) measurements were collected using an X'Pert X-ray powder diffractometer with an X'celerator detector. Samples were scanned at 45 kV and 40 mA using Co Kα radiation (λ = 1.789 Å) and a step size of 2θ = 0.02° (50.0 s/step) over a 2θ range of 3− 40°. Ar adsorption data were collected at 87 K using an Autosorb 2 from Quantachrome. Samples were outgassed at 200 $^oC$ overnight before the measurements. TGA measurements were obtained using a Shimadzu TGA-50 instrument. Samples were heated up to 700 $^oC$ (3 $^oC$ $min^{-1}$) under air flow (50 ml $min^{-1}$). DRIFTS spectra were recorded in a Nicollet spectrometer using an MCT detector with a spectral resolution of 2 $cm^{-1}$ and 256 scans. Around 30 mg of sample was packed in a bed and treated at 200 $^oC$ under Ar flow (50 mL $min^{-1}$) for 2 h before the recording. The SEM (Scanning Electron Microscopy) images were performed on a JEOL 6500 instrument at an accelerating voltage of 5kV. For the $^1H$ dissolution NMR experiments, about 20 mg of sample was weighed into an NMR tube. 600 µL of a 1M NaOH in $D_2O$ solution was added to the tube to digest the

samples. The mixture was let in contact for 24 h. Liquid $^{1}$H NMR spectra were recorded with a Bruker 400 MHz NMR spectrometer using 64 scans.

Catalytic evaluation of UiO-66: The catalytic reactions of UiO-66 were carried out at 90 ºC. In a typical reaction, 7 mg of catalyst, 5 mL of solvent and 0.04 g of D-glucose were added into a 20-mL thick-walled glass reactor and sealed with a crimp top (PTFE/silicone septum) from VWR. The reactor was placed in an oil bath. At specific reaction times, the reactor was quenched in an ice bath, and samples were collected. For the hydrolysis step, the catalyst was filtered out of the solution, and deionized water (5.00 g) was added to the solution, reacting for 24 h at 90 oC. The samples were analyzed by HPLC with a Bio-rad Aminex HPX87C (300 X 7.8 mm) column and refractive index detector. The mobile phase was ultrapure water (ph = 7.0) at 0.6 mL min$^{-1}$, and the column temperature was 80 ºC.

Isotopic labeling experiments: In the isotopic labeling experiments, reactions were conducted at 90 ºC using either D- [13C-C1, 1H-C2] or D-[13C-C1, 2H-C2]-glucose solutions for 24 h. The collected samples were evaporated in a rotavap and further dissolved in $D_2O$ for nuclear magnetic resonance (NMR) measurements. $^{1}$H NMR (32 scans) and $^{13}$C NMR (512 scans) spectra were collected using a Bruker 400 MHz NMR spectrometer.

Liquid adsorption experiments: A typical adsorption experiment involved mixing 10 mg of MOF with 250 µL of sugar solution (ranging from 0.01 to 1 wt%). The mixture was stirred for 24 h at 40 ºC followed by filtration (0.2 µm filter) for MOF removal. The amount of sugar present in solution after adsorption was determined by HPLC. The adsorption capacity (q, mg/g) was determined using the equation $q = {V(C_i - C_e)}/{m}$, where V is the initial volume of solution (mL), Ci and Ce are the initial and equilibrium concentrations of solute (mg mL-1), am m is the dry mass of zeolite (g) (i.e., neglecting the volume change caused by adsorption).

$^{13}$C Solid-state NMR experiments: Around 30 mg of MOF were mixed with 750 µL of 0.5 wt% sugar solution in 1-PrOH. The mixture was stirred for 24 h at 40 ºC, followed by centrifugation to separate the solid from the sugar solution. The powder was let to dry at room temperature overnight.

Solid-state, magic angle spinning nuclear magnetic resonance (MAS-NMR) measurements were performed using a Bruker Avance 700 MHz spectrometer equipped with an 11.7 T magnet and a Bruker 3.2 mm MAS probe. Samples of 30 mg powder were packed into 3.2 mm $ZrO_2$ rotors and spun at 10kHz for MAS experiments. 13C MAS-NMR (operating frequency 125.5 MHz) spectra were obtained with a recycle delay time of 5 s, and 10000 scans were accumulated for each sample. The CP transfer was achieved by fulfilling the Hartmann− Hahn matching condition. The first $^{1}$H 90° pulse was set to 5 µs. Finally, $^{1}$H 64-step small phase incremental alternation (SPINAL-64)68 decoupling was implemented during the acquisition period of the 13C NMR spectrum. The $^{13}$C chemical shifts were referenced to carbon signals in TMS.

## Acknowledgments

This work was supported as part of the Catalysis Center for Energy Innovation, an Energy Frontier Research Center funded by the U.S. Department of Energy, Office of Science, Basic Energy Sciences under Award DE-SC0001004. M.D.dM.'s doctoral fellowship was partially supported by the Brazillian National Council for Scientific and Technological Development (CNPq) under grant 202982/2014-9. The authors acknowledge the Minnesota NMR Center and in particular Dr. Gopinath Tata for performing the Solid-state NMR experiments.

**Keywords:** isomerization • glucose • UiO-66 • Lewis acid • metal-organic framework

[1] L. Wen, K. Huang, M. Wei, J. Meisner, Y. Liu, K. Garner, L. Zang, X. Wang, X. Li, J. Fang, et al., *Angew. Chemie - Int. Ed.* **2015**, *54*, 12654–12658.

[2] R. Van Putten, J. C. Van Der Waal, E. De Jong, C. B. Rasrendra, H. J. Heeres, J. G. De Vries, *Chem. Rev.* **2013**, *113*, 1499–1597.

[3] C. Sievers, I. Musin, T. Marzialetti, M. B. V. Olarte, P. K. Agrawal, C. W. Jones, *ChemSusChem* **2009**, *2*, 665–671.

[4] R. Karinen, K. Vilonen, M. Niemelä, *ChemSusChem* **2011**, *4*, 1002–1016.

[5] S. P. Simeonov, C. A. M. Afonso, *J. Chem. Educ.* **2013**, *90*, 1373–1375.

[6] T. D. Swift, H. Nguyen, Z. Erdman, J. S. Kruger, V. Nikolakis, D. G. Vlachos, *J. Catal.* **2016**, *333*, 149–161.

[7] X. Li, Q. Xia, V. C. Nguyen, K. Peng, X. Liu, N. Essayem, Y. Wang, *Catal. Sci. Technol.* **2016**, *6*, 7586–7596.

[8] M. Makkee, A. P. G. Kieboom, H. van Bekkum, *Recl. Trav. Chim. Pays-Bas* **1984**, *103*, 361–364.

[9] S. H. Bhosale, M. B. Rao, V. V Deshpande, *Microbiol. Rev.* **1996**, *60*, 280–300.

[10] A. A. Marianou, C. M. Michailof, A. Pineda, E. F. Iliopoulou, K. S. Triantafyllidis, A. A. Lappas, *ChemCatChem* **2016**, 1100–1110.

[11] M. Moliner, Y. Román-Leshkov, M. E. Davis, *Proc. Natl. Acad. Sci.* **2010**, *107*, 6164–6168.

[12] R. Bermejo-Deval, R. S. Assary, E. Nikolla, M. Moliner, Y. Román-Leshkov, S.-J. Hwang, A. Palsdottir, D. Silverman, R. F. Lobo, L. A. Curtiss, et al., *Proc. Natl. Acad. Sci.* **2012**, *109*, 9727–9732.

[13] R. Gounder, M. E. Davis, *J. Catal.* **2013**, *308*, 176–188.

[14] R. Gounder, M. E. Davis, *ACS Catal.* **2013**, *3*, 1469–1476.

[15] Y. Román-leshkov, M. Moliner, J. A. Labinger, M. E. Davis, *Angew. Chemie - Int. Ed.* **2010**, *49*, 8954–8957.

[16] M. Boronat, P. Concepción, A. Corma, M. Renz, S. Valencia, *J. Catal.* **2005**, *234*, 111–118.

[17] M. Boronat, A. Corma, M. Renz, *J. Phys. Chem. B* **2006**, *110*, 21168–21174.

[18] S. H. Mushrif, J. J. Varghese, C. B. Krishnamurthy, *Phys. Chem. Chem. Phys.* **2015**, *17*, 4961–4969.

[19] W. R. Gunther, Y. Wang, Y. Ji, V. K. Michaelis, S. T. Hunt, R. G. Griffin, Y. Román-Leshkov, *Nat. Commun.* **2012**, *3*, 1109–1117.

[20] H. Nguyen, V. Nikolakis, D. G. Vlachos, *ACS Catal.* **2016**, *6*, 1497–1504.

[21] G. Akiyama, R. Matsuda, H. Sato, S. Kitagawa, *Chem. - An Asian J.* **2014**, *9*, 2772–2777.

[22] H. Furukawa, K. E. Cordova, M. O'Keeffe, O. M. Yaghi, *Science* **2013**, *341*, 1230444.

[23] K. Leus, T. Bogaerts, J. De Decker, H. Depauw, K. Hendrickx, H. Vrielinck, V. Van Speybroeck, P. Van Der Voort, *Microporous Mesoporous Mater.* **2016**, *226*, 110–116.

[24] J. H. Cavka, S. Jakobsen, U. Olsbye, N. Guillou, C. Lamberti, S. Bordiga, K. P. Lillerud, *J. Am. Chem. Soc.* **2008**, *130*, 13850–13851.

[25] G. C. Shearer, S. Chavan, J. Ethiraj, J. G. Vitillo, S. Svelle, U. Olsbye, C. Lamberti, S. Bordiga, K. P. Lillerud, *Chem. Mater.* **2014**, *26*, 4068–4071.

[26] M. Kandiah, M. H. Nilsen, S. Usseglio, S. Jakobsen, U. Olsbye, M. Tilset, C. Larabi, E. A. Quadrelli, F. Bonino, K. P. Lillerud, *Chem. Mater.* **2010**, *22*, 6632–6640.

[27] J. Hajek, M. Vandichel, B. Van De Voorde, B. Bueken, D. De Vos, M. Waroquier, V. Van Speybroeck, *J. Catal.* **2015**, *331*, 1–12.

[28] D. Yang, S. O. Odoh, T. C. Wang, O. K. Farha, J. T. Hupp, C. J. Cramer, L. Gagliardi, B. C. Gates, *J. Am. Chem. Soc.* **2015**, *137*, 7391–7396.

[29] Y. Luan, Y. Qi, Z. Jin, X. Peng, H. Gao, G. Wang, *RSC Adv.* **2015**, *5*, 19273–19278.

[30] F. Vermoortele, B. Bueken, B. Van De Voorde, M. Vandichel, K. Houthoofd, A. Vimont, M. Daturi, M. Waroquier, V. Van Speybroeck, C. E. a Kirschhock, et al., *J. Am. Chem. Soc.* **2013**, *135*, 11465–11468.

[31] R. Oozeerally, D. L. Burnett, T. W. Chamberlain, R. I. Walton, V. Degirmenci, *ChemCatChem* **2017**, DOI 10.1002/cctc.201701825.

[32] J. Chen, K. Li, L. Chen, R. Liu, X. Huang, D. Ye, *Green Chem.* **2014**, *16*, 2490–2499.

[33] F.-G. Xi, Y. Yang, H. Liu, H.-F. Yao, E.-Q. Gao, *RSC Adv.* **2015**, *5*, 79216–79223.

[34] G. C. Shearer, S. Chavan, S. Bordiga, S. Svelle, U. Olsbye, K. P. Lillerud, *Chem. Mater.* **2016**, *28*, 3749–3761.

[35] M. J. Katz, Z. J. Brown, Y. J. Colón, P. W. Siu, K. a Scheidt, R. Q. Snurr, J. T. Hupp, O. K. Farha, *Chem. Commun.* **2013**, *49*, 9449–9451.

[36] M. Vandichel, J. Hajek, F. Vermoortele, M. Waroquier, D. E. De Vos, V. Van Speybroeck, *CrystEngComm* **2014**, *17*, 395–406.

[37] D. Yang, S. O. Odoh, J. Borycz, T. C. Wang, O. K. Farha, J. T. Hupp, C. J. Cramer, L. Gagliardi, B. C. Gates, *ACS Catal.* **2016**, *6*, 235–247.

[38] L. Valenzano, B. Civalleri, S. Chavan, S. Bordiga, M. H. Nilsen, S. Jakobsen, K. P. Lillerud, C. Lamberti, *Chem. Mater.* **2011**, *23*, 1700–1718.

[39] L. Ren, Q. Guo, P. Kumar, M. Orazov, D. Xu, S. M. Alhassan, K. A. Mkhoyan, M. E. Davis, M. Tsapatsis, *Angew. Chemie - Int. Ed.* **2015**, *54*, 10848–10851.

[40] C. D. Malonzo, S. M. Shaker, L. Ren, S. D. Prinslow, A. E. Platero-Prats, L. C. Gallington, J. Borycz, A. B. Thompson, T. C. Wang, O. K. Farha, et al., *J. Am. Chem. Soc.* **2016**, *138*, 2739–2748.

[41] S. Saravanamurugan, M. Paniagua, J. A. Melero, A. Riisager, *J. Am. Chem. Soc.* **2013**, *135*, 5246–5249.

[42] A. I. Torres, P. Daoutidis, M. Tsapatsis, *Energy Environ. Sci.* **2010**, *3*, 1560–1572.

[43] I. Delidovich, R. Palkovits, *ChemSusChem* **2016**, *9*, 547–561.

[44] M. J. King-Morris, A. S. Serianni, *J. Am. Chem. Soc.* **1987**, *109*, 3501–3508.

[45] G. Zhang, P. Feng, W. Zhang, H. Liu, C. Wang, H. Ma, D. Wang, Z. Tian, *Microporous Mesoporous Mater.* **2017**, *247*, 158–165.

[46] S. Devautour-Vinot, G. Maurin, C. Serre, P. Horcajada, D. Paula Da Cunha, V. Guillerm, E. De Souza Costa, F. Taulelle, C. Martineau, *Chem. Mater.* **2012**, *24*, 2168–2177.

[47] K. N. Drew, J. Zajicek, G. Bondo, B. Bose, A. S. Serianni, *Carbohydr. Res.* **1998**, *307*, 199–209.

[48] W. N. P. van der Graaff, C. H. L. Tempelman, G. Li, B. Mezari, N. Kosinov, E. A. Pidko, E. J. M. Hensen, *ChemSusChem* **2016**, *9*, 3145–3149.

[49] X. Qian, X. Wei, *J. Phys. Chem. B* **2012**, *116*, 10898–10904.

[50] B. Tang, W. Dai, G. Wu, N. Guan, L. Li, M. Hunger, *ACS Catal.* **2014**, *4*, 2801–2810.

[51] J. Tang, X. Guo, L. Zhu, C. Hu, *ACS Catal.* **2015**, *5*, 5097–5103.

[52] S. Saravanamurugan, A. Riisager, E. Taarning, S. Meier, *ChemCatChem* **2016**, *8*, 3107–3111.

[53] T. W. Bentley, I. S. Koo, H. Choi, G. Llewellyn, *J. Phys. Org. Chem.* **2008**, *21*, 251–256.

10.1002/cctc.201800371

WILEY-VCH



**Entry for the Table of Contents**
Layout 1:

## FULL PAPER

A modified zirconium UiO-66 is shown to be a highly active catalyst for glucose isomerization to fructose. We report fructose selectivities in different solvents. The catalyst matches the performance of optimized Lewis acid zeolites. The reaction follows an intramolecular hydride transfer mechanism.

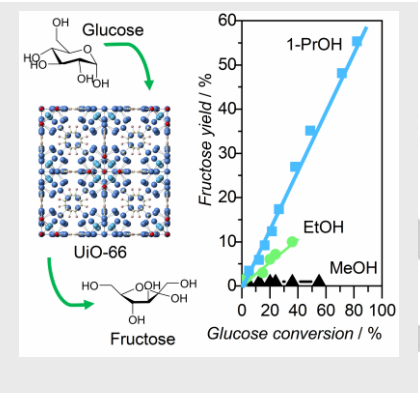


*Matheus Dorneles de Mello, Michael Tsapatsis**

***Page No. – Page No.***

**Selective glucose to fructose isomerization over modified zirconium UiO-66 in alcohol media**